Electronic Supplementary Information:

Facile One-Pot Synthesis of Multi-Yolk-Shell Bi@C Nanostructures by the Nanoscale Kirkendall Effect

Chengmei Cui, Xiaohui Guo*, Yanmin Geng, Taotao Dang, Gang Xie*, Sanping Chen, Fengqi Zhao

EXPERIMENTAL SECTION:

Materials:

Glucose ($C_6H_{12}O_6$), glacial acetic acid (CH_3COOH), bismuth nitrate pentahydrate ($Bi(NO_3)_3$• $5H_2O$) and polyvinylpyrrolidone (PVP-K30) were obtained from Sinopharm. Cyclotrimethylenetrinitramine (RDX) used in this study was purchased from Baiyin Chemical Engineering Factory. All chemicals were analytical grade and used as received without further purification.

Synthesis of Bi@C multi-yolk-shell Nanostructures

In a typical process, 0.6 g of $C_6H_{12}O_6$, 0.2 g of $Bi(NO_3)_3$ • $5H_2O$ and 0.1g of surfactant PVP-K30 were dissolved in 2 mL of deionized water under magnetic stirring to form a transparent solution. Afterward, 1 mL of CH_3COOH was added into the above homogeneous solution with vigorous stirring simultaneously. 20 min later, the resultant solution was transferred into a 10 mL Teflon-lined stainless steel autoclave. Then, the autoclave was heated from room temperature to 200 ^oC with a heating rate of 5 ^oC /min and maintained at 200 ^oC for 1h. After the autoclave was allowed to cool to room temperature, the black products were separated centrifugally and washed several times with deionized water and absolute ethanol several times. Finally, the products were dried under vacuum oven at 60 ^oC for 6 h. The time-dependent or glucose-controlled experiments were prepared as same the above, except that the corresponding reaction time or the amounts of glucose are changed.

Characterization:

Phase composition of the prepared Bi@Carbon structures was monitored by X-ray diffraction (XRD) on a Bruker D8 diffractometer operated at 40 kV and 40 mA using Cu-Kα radiation (λ = 0.15418 nm) by scanning from 2θ = 10 to 80º. Sample morphology was recorded via Scanning electron microscopy (SEM) on a Jeol JSM-6390A field emission scanning electron microscope (FESEM). Transmission electron microscopy (TEM, Philips Tecnai G2 F20) was investigated with an accelerating voltage of 200 KV that equipped with energy-dispersive spectroscopy (EDS). Raman spectra was taken via using a Raman spectrometer (Jobin Yvon Co., France) model HR800 employing a 10 mW helium/neon laser at 632.8 nm.

Combustion catalytic test:

The combustion catalytic activity of the samples was evaluated by the thermal decomposition of RDX powder. Both the mixture Bi@C-RDX (mass ratio, 1/2) and pure RDX were analyzed in a NETZSCH-Proteus DSC-404F3 instrument. The catalytic conditions of DSC were as follows: sample mass is less than 2.00 mg; heating rates are 5, 10, 15 and 20 $^oC\ min^{-1}$; atmosphere pressure is 0.1 MPa, a flowing rate of N_2 gas is 50 ml min^{-1}.

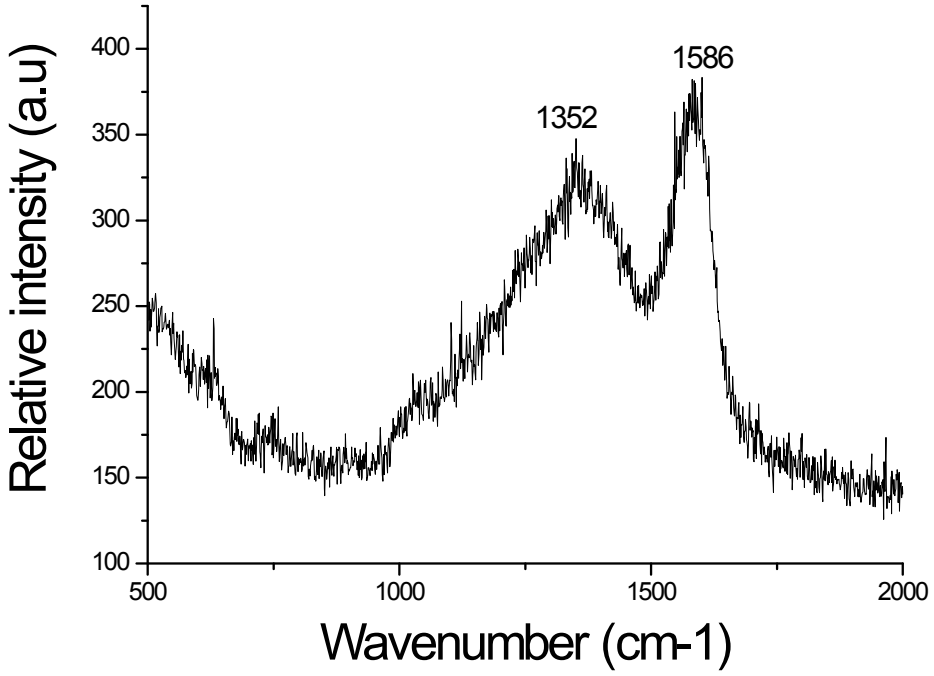

Figure S1: Raman spectroscopy of the prepared Bi@C yolk-shell sample.

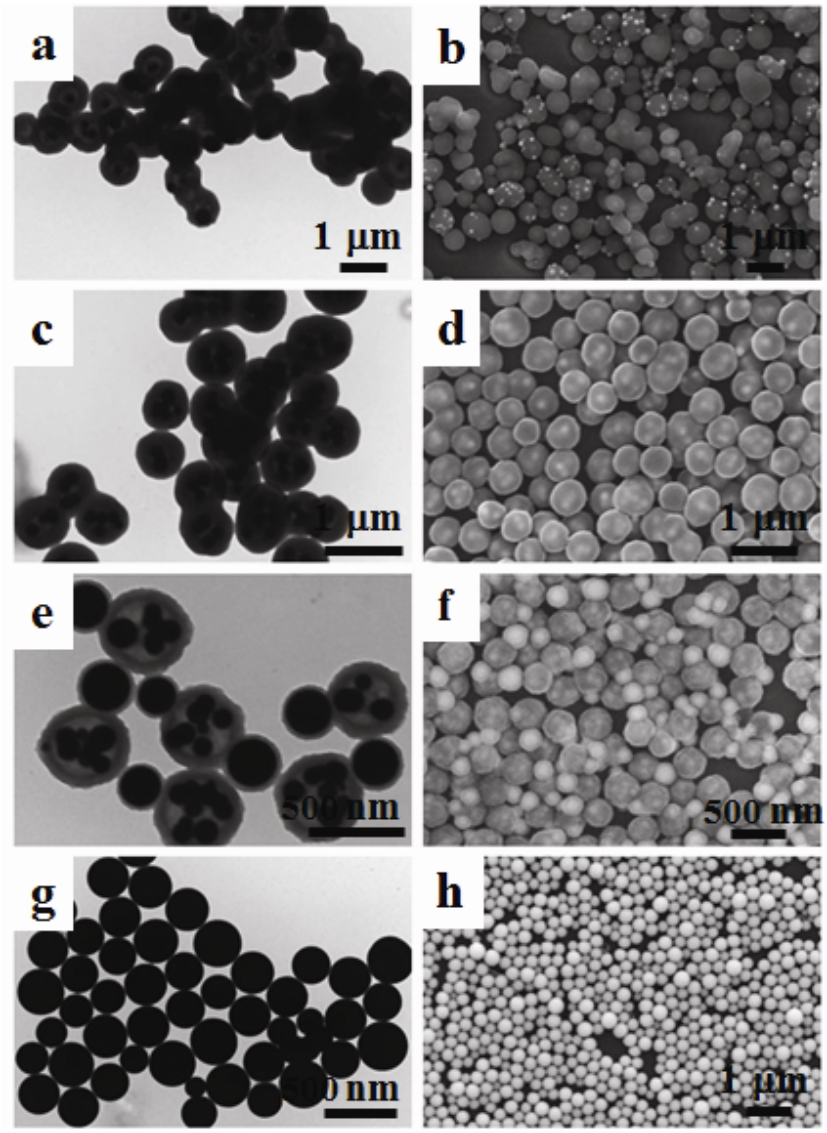

Figure S2. TEM and SEM images of the synthesized products at 200 °C hydrothermal reaction for 1h with different amounts of glucose: (a, b) 1.5 g; (c, d) 1.0 g; (e, f) 0.4 g; (g, h) 0.1 g of glucose, respectively.

While increasing the amounts of glucose to 1.5 g, the thickness of carbon layer increases and the surface roughness of the product decrease (Figure S2a and b). In addition, the number of Bi particles in each carbon shell also decreases or even disappears. Interestingly, peanut-like structures are formed in the case of 1.0 g glucose owing to the adhesion of two adjacent particles (Figure S2c and d). On the contrary, the thickness of carbon layer decreases and the surface roughness of the product increase while the amounts of glucose were further decreased. Interestingly,

a class of Cucurbit-like Bi@C heterodimers can be formed in the presence of 0.4 g glucose (Figure S2e and f). When the amount of glucose was decreased to 0.1 g, monodispersed metallic Bi spheres with a size ranging from 250 to 480 nm could be prepared, it was observed that there no carbon layer capping on the surface of the solid particle (Figure S2g and h).

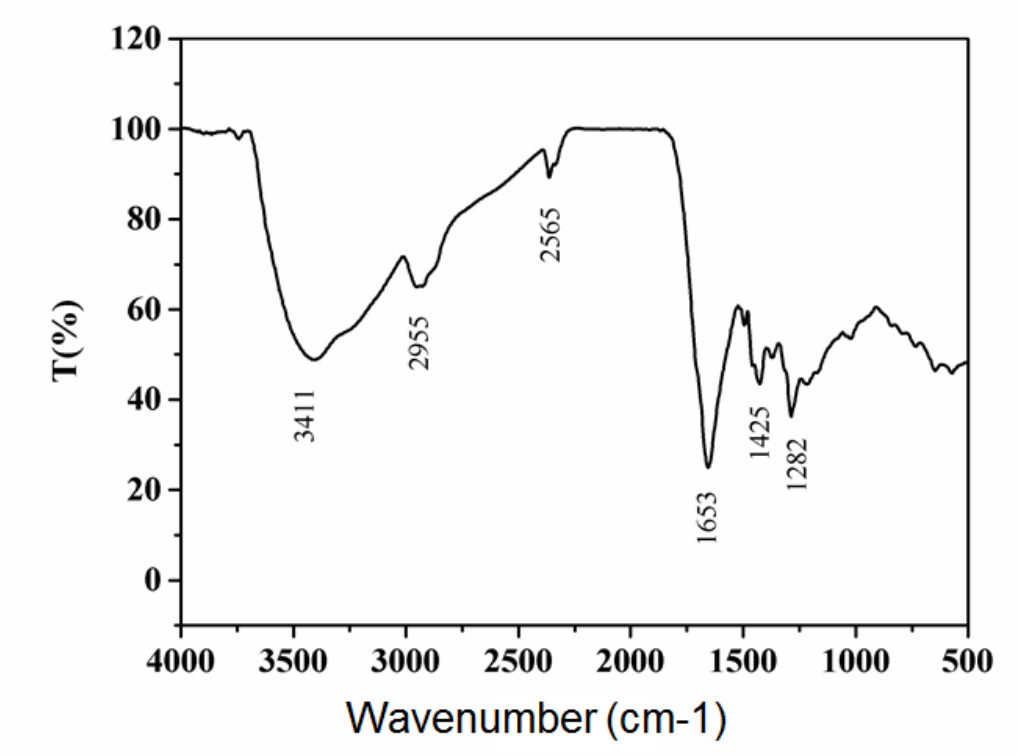

Figure S3: FTIR result of the prepared Bi@C sample

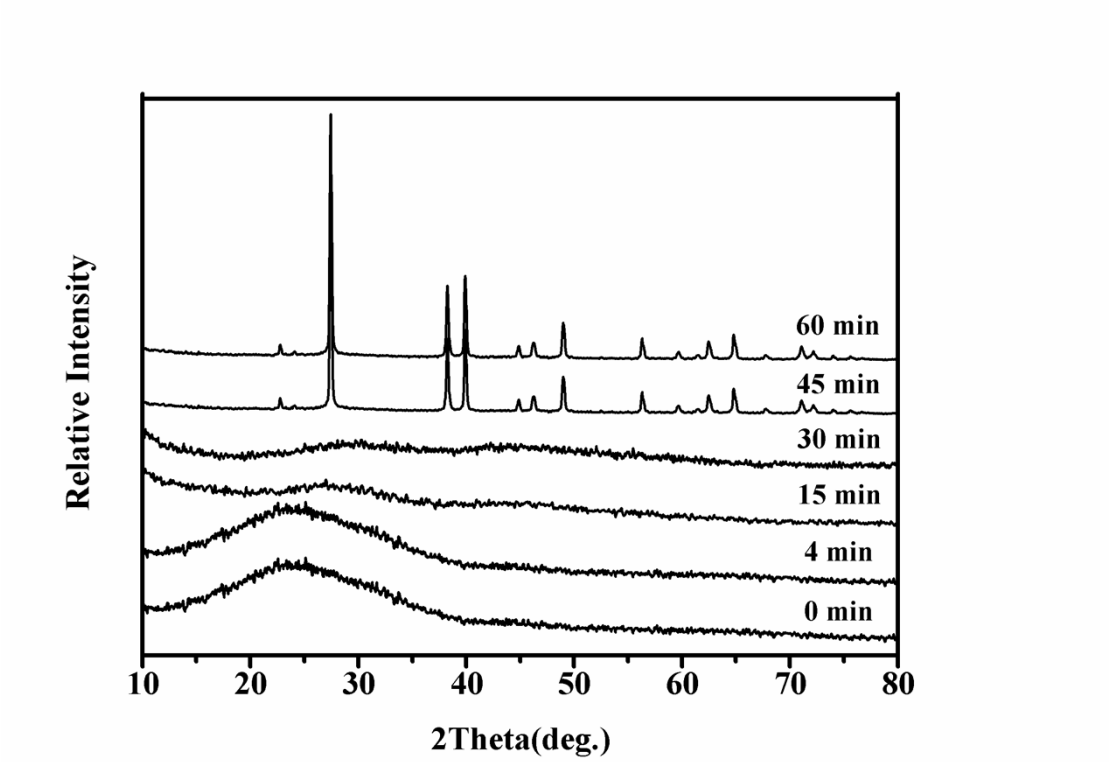

Figure S4. XRD patterns of Bi@C (0.6 g glucose) composites obtained at 200 ^{o}C hydrothermal reaction for different reaction times.

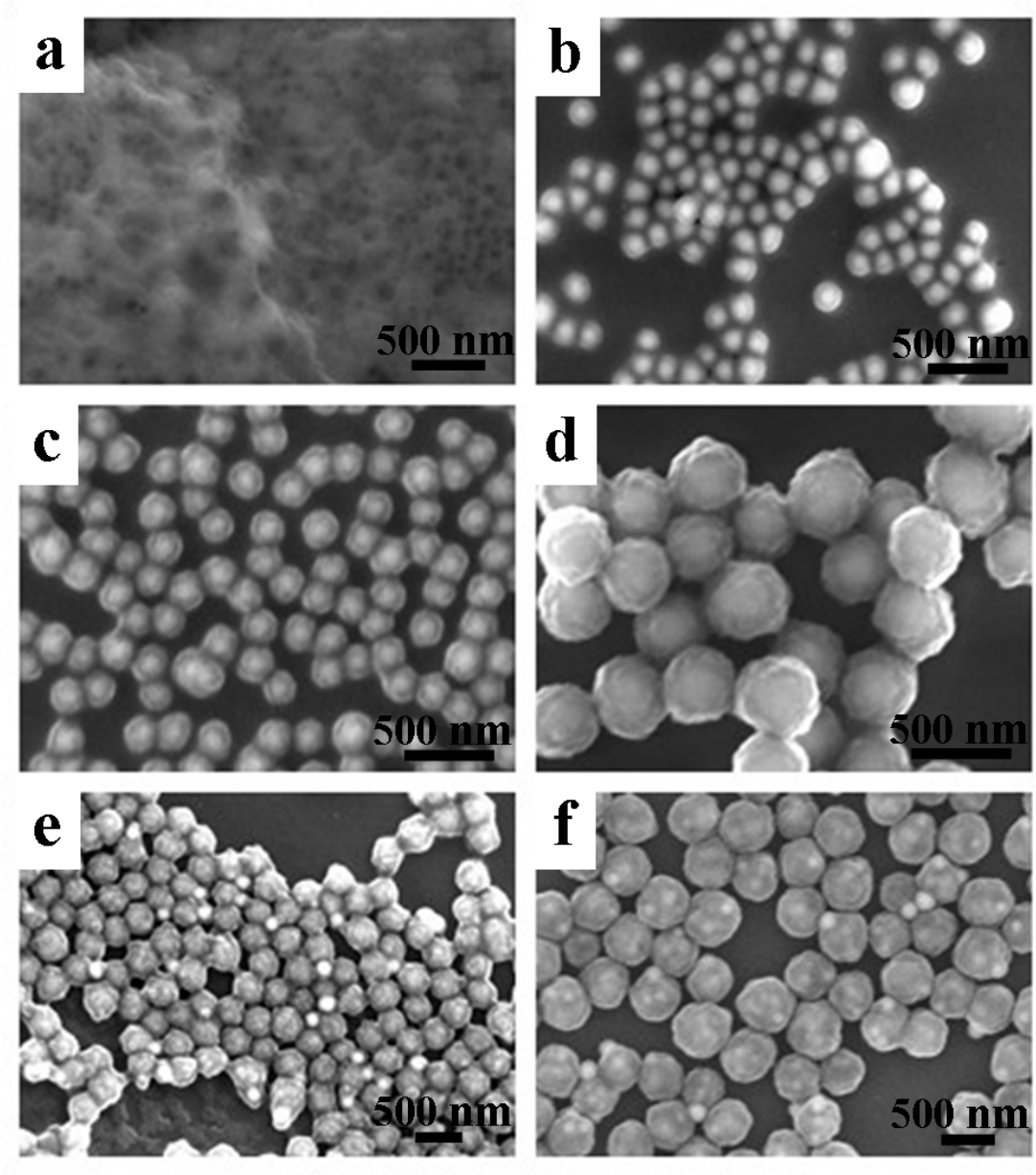

Figure S5. SEM images of Bi@C (0.6 g glucose) samples synthesized at 200 °C hydrothermal reaction for (a) 0, (b) 4, (c) 15, (d) 30, (e) 45, and (f) 60 min, respectively. Other reaction parameters are kept constant.

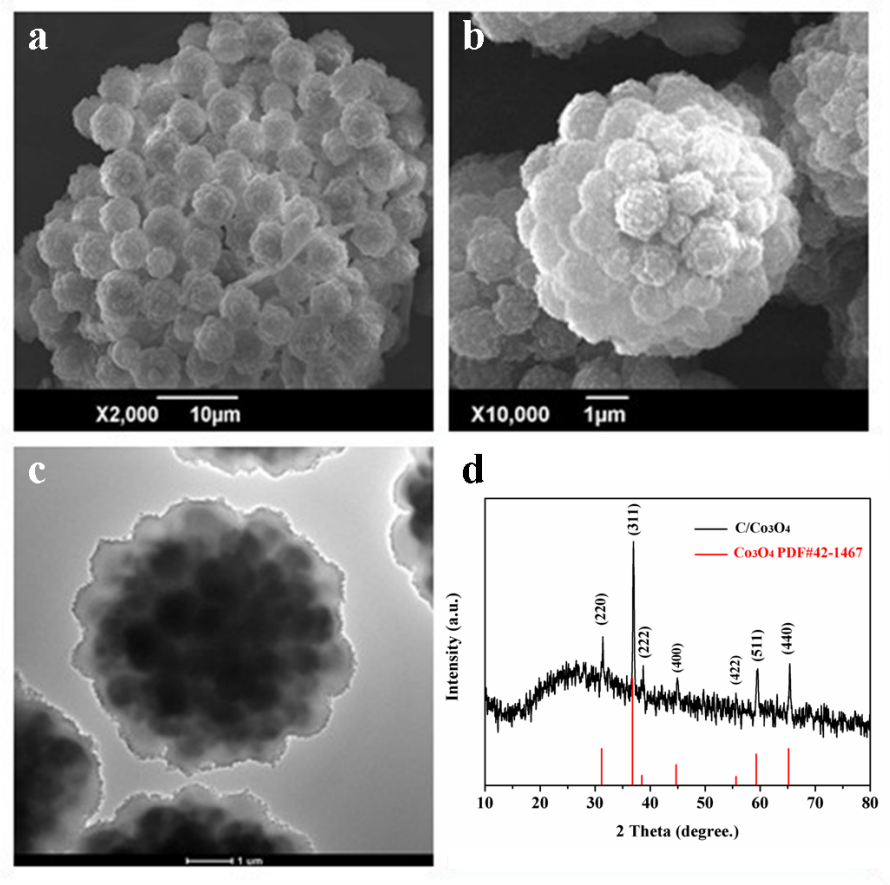

Figure S6: Morphology and structure analysis for the prepared flower-like C/Co_3O_4 core-shell structure, (a, b) SEM image; (c) TEM image; (d) XRD pattern

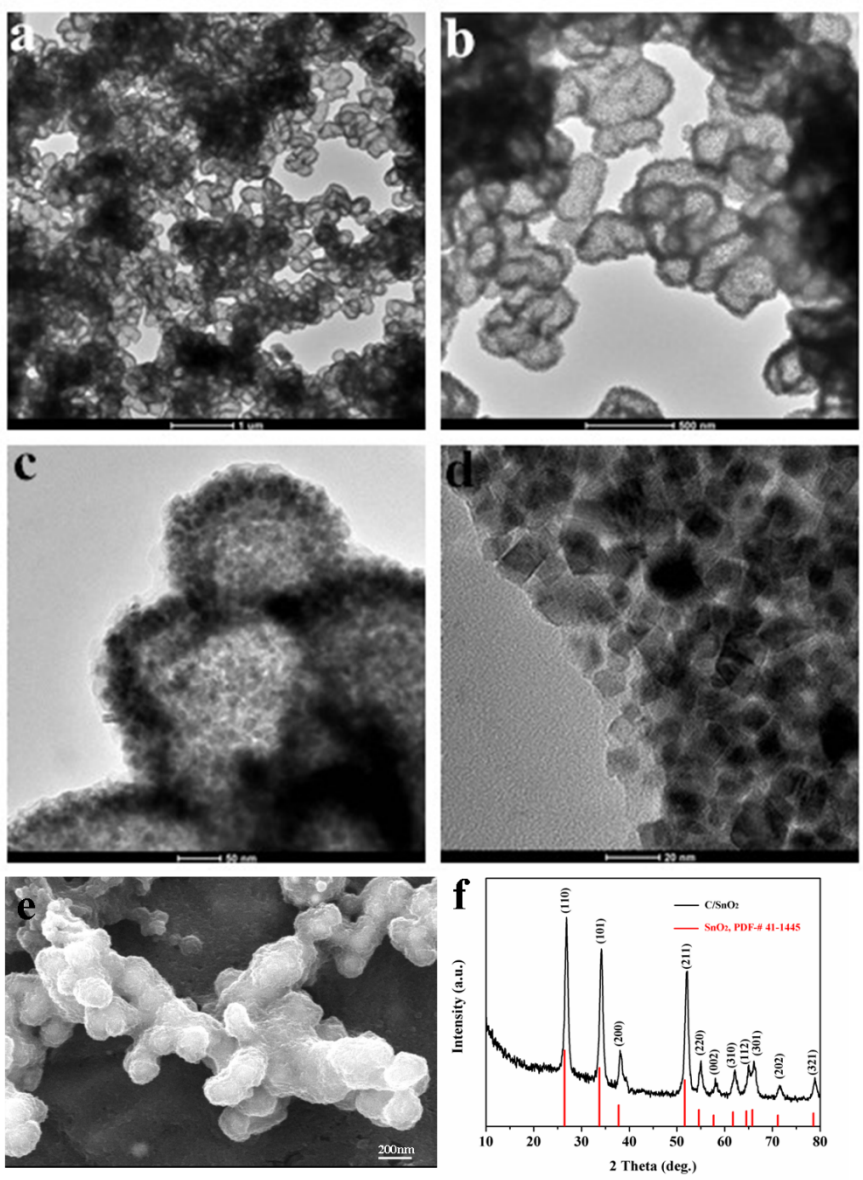

Figure S7: Morphology and structure analysis for the prepared hollow C/SnO_2 composite, (a, b, c and d) TEM images with different magnifications; (e) SEM image; (f) XRD pattern.

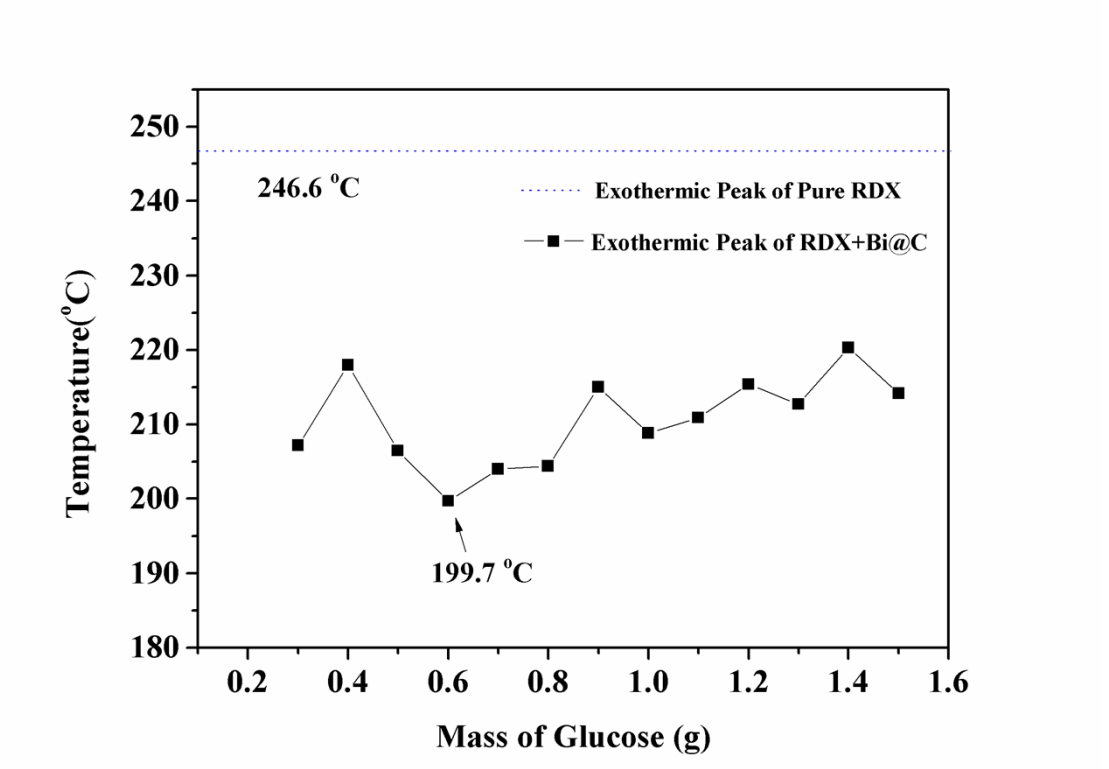

Figure S8. Exothermic decomposition temperature curves of RDX mixed with Bi@C samples obtained with different amounts of glucose, in which, heating rate is 15 K min^{-1}.

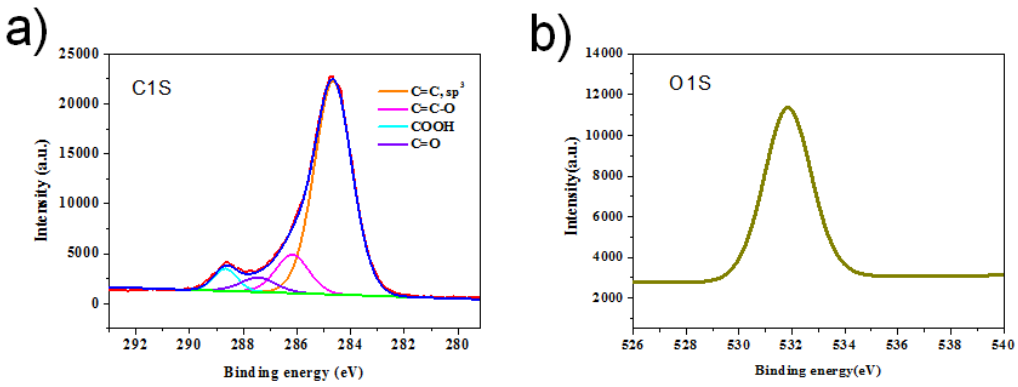

Figure S9: XPS spectra of the prepared sample, a) C1S; b) O1S.

Table 1: Summary of the C1S XPS data

Group types	**BE(eV)**	**At. %**
C=C, sp^3	284.66	77.56
C=C-O	286.18	12.32
COOH	288.67	5.11
C=O	287.44	5.01

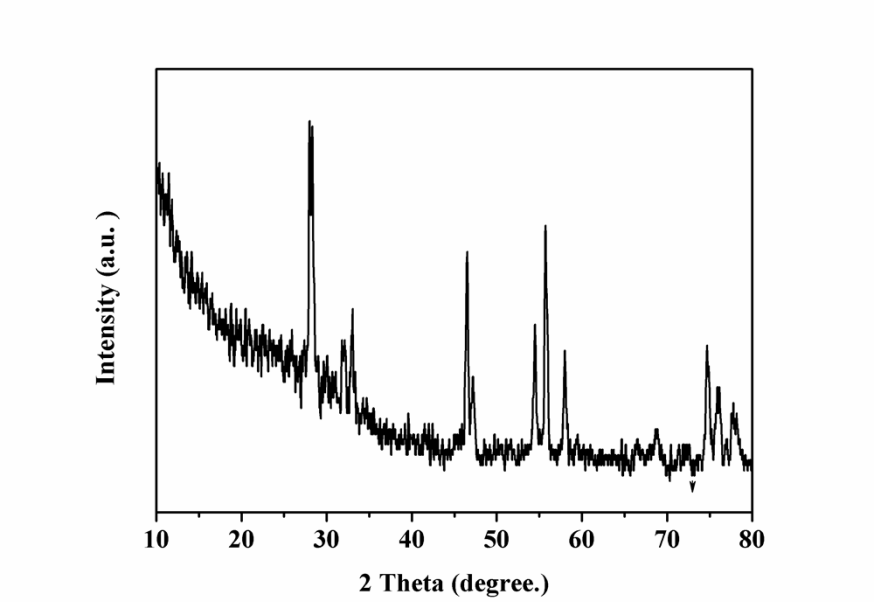

Figure S10: XRD pattern of the thermal decomposition product of RDX.

Table 2 DSC Parameters of samples at different heating rates

Samples	β/℃ min^{-1}	Endothermic peaks				Exothermic peaks			
		T_o/℃	T_p/℃	T_e/℃	△H_1/J g^{-1}	T_o/℃	T_p/℃	T_e/℃	△H_2/J g^{-1}
RDX	5	202.9	203.8	205.5	96.4	205.9	234.10	243.5	1051
	10	203.8	205.0	206.8	75.17	207.1	245.94	256.2	1642
	15	203.8	205.0	207.2	60.83	209.4	253.79	263.8	1687
	20	203.8	205.1	207.9	60.38	215.1	255.06	269.2	1623
RDX$_{1/7}$	5	201.6	202.9	205.2	15.89	205.4	219.93	228.2	978.25
	10	201.8	203.1	204.9	20.86	205.8	227.44	241.0	751.33
	15	200.9	202.7	206.1	30.49	206.6	235.97	248.5	773.5
	20	201.4	203.2	208.3	25.61	208.7	241.52	257.1	855.17
RDX$_{1/5}$	5	-	-	-	-	200.9	212.14	222.4	865
	10	-	-	-	-	202.5	221.96	237.7	1116.25
	15	200.9	202.3	203.5	13.69	203.7	228.97	243.9	1068.5
	20	200.9	202.6	204.1	13.23	206.1	234.30	250.9	1039.63
RDX$_{1/3}$	5	-	-	-	-	185.4	192.24	201.1	785.4
	10	-	-	-	-	192.2	199.71	219.1	1392.45
	15	199.7	201.5	205.0	16.59	205.1	219.41	232.7	1028.4
	20	199.4	201.6	208.2	21.50	208.3	222.52	237.6	978.15

β – heating rate; T_o–onset temperature; T_p–peak temperature; T_e–end temperature; △H_1–heat absorption; △H_2–heat release.

Table 3 Kinetic parameters of samples from non-isothermal DSC data

Samples	Kissinger method			Ozawa method	
	E_{aK}/kJ mol^{-1}	lg(A/s^{-1})	r_K	E_{aO}/kJ mol^{-1}	r_O
RDX	137.72	13.68	0.9909	140.50	0.9989
RDX$_{1/7}$	123.43	12.60	0.9786	125.54	0.9983
RDX$_{1/5}$	118.93	12.30	0.9972	121.95	0.9987
RDX$_{1/3}$	66.53	5.02	0.9441	70.86	0.9548

E_a–apparent activation energy; A – Pre-exponential factor; the subscript K and O indicate that the parameters were calculated by the Kissinger and Ozawa methods, respectively; r – linear correlation coefficient.